

Stokes flow past a pair of stagnant-cap bubbles

By L. LERNER† AND J. F. HARPER‡

Mathematics Department, Victoria University of Wellington, New Zealand

(Received 11 June 1990 and in revised form 26 February 1991)

When gas bubbles rise in a surface-contaminated liquid, the upper parts of their surfaces may be almost free of contaminant and shear stress, while on the remainder of their surfaces there is enough contaminant to prevent tangential motion. Sadhal & Johnson solved the problem of Stokes flow of a uniform stream past a single spherical bubble. We extend their method to a single bubble in an arbitrary axially symmetric Stokes flow with the aid of an inversion theorem due to Harper. We also investigate in detail the interaction between two bubbles rising in line, and show how the methods can be made to deal with three or more bubbles, or a line of one or more bubbles rising towards a free surface. We show that a pair of bubbles will remain the same distance apart only if there is a certain relationship between the sizes of the caps on the bubbles. The cap sizes will normally be determined by convective diffusion of a surface-active solute from the bulk liquid in which the bubbles rise. The position of the lower bubble vertically under the upper one is stable to small horizontal displacements, but the upper bubble rises faster and so the distance apart gradually increases.

1. Introduction

The interaction of small liquid drops or bubbles rising in a viscous fluid is an area of fluid dynamics which has attracted much interest in the past (Clift, Grace & Weber 1978; Harper 1972, 1983; Pruppacher & Klett 1978). It has applications in such areas as chemical engineering and meteorology where one deals with the motion of many small drops whose radii are comparable to their separation. Their interaction at such short separations can have consequences important to the behaviour of the fluid as a whole. We treat not the general problem but a very special case in which the underlying physics is as clear as possible: a pair of bubbles rising in a vertical line, with both in Savic's stagnant-cap regime.

In treating viscous axisymmetric flow at low Reynolds number Re , approximations can be made in the Navier–Stokes equations resulting in the Stokes differential equation of motion which is known to give good agreement for flows with $Re \ll 1$. Stokes' equation, with the appropriate boundary conditions, has been applied in the past to the motion of drops and bubbles in a viscous fluid, and their interactions have been calculated for a number of cases both for tangentially stress-free surfaces (Wacholder & Weihs 1972; Harper 1983) and for rigid surfaces (Davis *et al.* 1976; Rushton & Davies 1978). Depending on the amount of surface-active material (surfactant) dissolved in the fluid, either case can apply; see, for example, Harper

† Present address: Research School of Physical Sciences, Australian National University, GPO Box 4, Canberra, ACT 2601, Australia.

‡ Author to whom correspondence should be sent.

(1972, 1982) and Clift *et al.* (1978) for reviews of the extensive literature. If surfactant is present, but there is not enough of it to stop surface motion on the whole bubble, Savić (1953) showed that it could clog a region whose shape is a spherical cap on the bottom of the rising bubble (the stagnant cap) while the remainder of the bubble is tangentially stress-free. The word 'clog' is not meant to convey that surfactant molecules form a close-packed monolayer on the surface, only that through the tangential gradient of their surface concentration they create surface shear sufficient to prevent surface motion.

This problem for one isolated sphere in an otherwise uniform stream has been dealt with theoretically by Savić (1953), Davis & Acrivos (1966), Harper (1973) and most recently by Sadhal & Johnson (1983, hereinafter referred to as SJ), who produced an exact solution, showed why the transition from free to clogged surface is very sudden (as had been found by Harper & Dixon (1974) for the case of a plane surface with a stream flowing at high Reynolds number beneath), and concluded that it is a good approximation for low-Reynolds-number and high-Péclet number flows (so that diffusion boundary layers are thin).

Our aim is to extend the problem to interactions of such drops or bubbles with arbitrary sized caps by solving it for the case of two bubbles, with equal radii, moving parallel to their line of centres in Stokes flow in a fluid at rest at infinity. The same method also deals with three or more bubbles, or with one bubble rising towards a plane free surface, as outlined in §3.6. We deal with a stagnant-cap bubble in any axisymmetric Stokes flow by writing the stream function in a Legendre series in spherical polar coordinates, using SJ to reduce the problem to that of a capless bubble in the same Stokes flow, and solving that by the inversion theorem of Harper (1983). We do not consider in this paper a pair of drops with non-negligible interior viscosity, because the analogue of Harper (1983) for capless drops would be much more complicated. The method of reflections then enables us to satisfy the boundary conditions on two bubbles. We also briefly mention a second method, which consists of expanding the stream function in series in bispherical coordinates. We checked each calculation by its agreement with the other. Another reason for doing both calculations is that they generalize readily in different ways: the first to more bubbles, the second to two drops whose interior viscosity can be comparable to that of the external fluid. We avoided a conventional boundary-integral method in order to take advantage of the precise treatment of the singularities at the edges of the caps in SJ.

In §2 we set up the notation and present some preliminary results. In §3 we use the method of reflections to obtain an infinite-dimensional matrix equation for the solution. We show that the matrix equation can be truncated and that good convergence can be obtained when calculating the drag, if the ratio of bubble centre separation to radius is greater than 2.4. If the ratio is small enough and the caps are large enough, back-eddies form between the bubbles and our solution is not physically valid, because there are then several zones of free and clogged surface. Davis *et al.* (1976) found that eddies appear for ratios less than 3.57 if the caps completely cover both bubbles; the minimum ratio for eddies to form decreases as the cap sizes decrease. Section 4 discusses the consequences of the stagnant caps being maintained by convective diffusion, including stability to small sideways displacement of the second bubble but instability to larger displacements. Section 5 gives the conditions for validity of the analysis, including an example to check that they can all be satisfied together. In §6 we give results for the stream functions and forces on the bubbles as functions of their cap size and separation. We also check for

vertical instability by finding the relationship between the cap angles of the bubbles required to produce steady flow. At least for small caps or widely separated bubbles, this relationship is not the one imposed by convective diffusion of the surfactant. As a result the second bubble rises more slowly than the first. The equal-drag relationship between the cap angles is also not the simple one that might have been expected intuitively; in fact the difference between cap sizes possesses three extrema. Sections 2, 3 and parts of 6 are based on an unpublished thesis of Lerner (1985).

2. Preliminaries

2.1. Coordinates

Let \mathbf{x} be the position vector from the centre of the first (topmost) rising bubble,

$$r = |\mathbf{x}|, \quad \mu = \cos \theta = \mathbf{k} \cdot \mathbf{x} / r, \tag{1}$$

where \mathbf{k} is a unit vector pointing vertically downwards, so that (r, θ) are spherical polar coordinates with $\theta = 0$ pointing downstream. Let the vector $\mathbf{x}' = \mathbf{x} - s\mathbf{k}$, so that \mathbf{x}' is zero at a distance s below the centre of the first bubble, and let (r', θ') be spherical polar coordinates centred there, i.e.

$$r' = |\mathbf{x}'| = (r^2 - 2rs \cos \theta + s^2)^{\frac{1}{2}}, \tag{2}$$

$$\mu' = \cos \theta' = \mathbf{k} \cdot \mathbf{x}' / r', \tag{3}$$

$$r' \sin \theta' = r \sin \theta, \quad r' \mu' = r\mu - s. \tag{4}$$

Usually the surfaces of two bubbles will be taken as $r = 1, r' = 1$ in what follows.

2.2. Motion of a single bubble

In this section we introduce the notation which we use and the SJ solution which we generalize. Consider the axisymmetric flow of a uniform stream of liquid of dynamic viscosity η at speed U past a single spherical bubble at $r = 1$. The approximation of the bubble's surface to that of a sphere will be good if the capillary number $\eta U / \sigma$ is small, i.e. the surface tension σ is high enough to dominate viscous forces, and if σ varies only slightly around the bubble, in a sense which is made more explicit in § 5 below. The surfactant accumulates at the rear of the bubble producing a stagnant cap of angular size α . Subtracting the flow at infinity, we get the equivalent problem of the rise of a spherical bubble in fluid otherwise at rest.

SJ gave the exact solution to the above problem in terms of the usual stream function Ψ which is used to define velocity components u_r, u_θ satisfying the continuity equation:

$$u_r = \frac{1}{r^2 \sin \theta} \frac{\partial \Psi}{\partial \theta}, \quad u_\theta = -\frac{1}{r \sin \theta} \frac{\partial \Psi}{\partial r} \quad (1 < r < \infty); \tag{5}$$

the differential equation for Stokes flow is

$$D^2 \Psi = 0, \quad D = \frac{\partial^2}{\partial r^2} + \frac{1 - \mu^2}{r^2} \frac{\partial^2}{\partial \mu^2}. \tag{6}$$

If we define $\phi_k(r, \mu) = r^{-k} I_k(\mu)$ and $\psi_k(r, \mu) = r^{2-k} I_k(\mu)$, where

$$I_k(\mu) = \int_\mu^1 P_k(x) dx = \frac{1 - \mu^2}{k(k+1)} \frac{dP_k(\mu)}{d\mu} = \frac{P_{k-1}(\mu) - P_{k+1}(\mu)}{2k+1}, \tag{7}$$

we also have $D\phi_k = 0$ and

$$D\psi_k = (2-4k)\phi_k \quad (8)$$

so that $D^2\psi_k = 0$, and there is a solution

$$\Psi = \Psi_U + U\chi^*(0, \alpha) = \Psi_U + \mathcal{J}(0, 1)\Psi_U + U\chi(0, \alpha) \quad (9)$$

to the Stokes equation, where $\Psi_U = Ur^2/I_1(\mu)$ is the stream function of the uniform stream, $\mathcal{J}(s, a)\Psi_U$ is its inverse (Harper 1983) in the sphere with centre at s and radius a , so that

$$\mathcal{J}(0, a)\Psi(r, \theta) = -(r^3/a^3)\Psi(a^2/r, \theta), \quad (10)$$

and

$$\chi^*(0, \alpha) = \sum_{k=1}^{\infty} (C_k^* \psi_k - C_k \phi_k), \quad \chi(0, \alpha) = \sum_{k=1}^{\infty} C_k (\psi_k - \phi_k), \quad (11)$$

where $C_k^* = C_k - \delta_{1k}$. Although ϕ_k, ψ_k are not orthogonal with any inner product we find useful, they are linearly independent and we term them basis functions. We also define functions singular at $r' = 0$ as

$$\begin{aligned} \phi'_k &= \phi_k(r', \mu'), & \psi'_k &= \psi_k(r', \mu'), \\ \chi^*(s, \alpha) &= \sum_{k=1}^{\infty} (C_k^* \psi'_k - C_k \phi'_k), & \chi(s, \alpha) &= \sum_{k=1}^{\infty} C_k (\psi'_k - \phi'_k). \end{aligned}$$

The boundary conditions appropriate to the capped bubble are

$$\Psi \sim \frac{1}{2}Ur^2 \sin^2 \theta \quad (r \rightarrow \infty, \quad 0 \leq \theta \leq \pi) \quad (12)$$

$$\Psi = 0 \quad (r = 1, \quad 0 \leq \theta \leq \pi) \quad (13)$$

$$\frac{\partial \Psi}{\partial r} = 0 \quad (r = 1, \quad 0 \leq \theta < \alpha) \quad (14)$$

$$p_{r\theta} = 0 \quad (r = 1, \quad \alpha < \theta \leq \pi), \quad (15)$$

where $p_{r\theta} = (\eta/\sin \theta) \partial^2 \Psi / \partial r^2$ on the surface, η is the dynamic viscosity of the fluid outside the bubble, and $\Psi = \partial \Psi / \partial r = 0$. The coefficients C_k were obtained by SJ and are given by

$$C_k = \frac{1}{4\pi} \left(\frac{k}{k+2} \sin(k+2)\alpha + \sin(k+1)\alpha - \sin k\alpha - (k+1)S_k \right) \quad (16)$$

where

$$S_k = \frac{\sin(k-1)\alpha}{k-1} \quad (k \geq 2),$$

$$S_1 = \alpha. \quad (17)$$

To obtain (16), SJ used a method due to Collins (1961) for solving the system of dual series equations given below. We repeat it here in the form that we use. If $f(\theta)$ is such that $f(\theta)/\sin \theta$ is continuous on the domain $[0, \pi]$, the equations

$$\sum_{k=1}^{\infty} c_k I_k(\cos \theta) = f(\theta) \quad (0 \leq \theta < \alpha), \quad (18)$$

$$\sum_{k=1}^{\infty} c_k (2k+1) I_k(\cos \theta) = 0 \quad (\alpha < \theta \leq \pi), \quad (19)$$

have the unique solution

$$c_k = \int_0^\alpha h(u) (k \sin(k+1)u + (k+1) \sin ku) du, \quad (20)$$

where

$$h(u) = \frac{1}{\sqrt{2\pi \sin(\frac{1}{2}u)}} \frac{d}{du} \int_0^u \frac{f(\theta) \sin \theta d\theta}{(\cos \theta - \cos u)^{\frac{1}{2}} (1 + \cos \theta)}. \quad (21)$$

3. Stokes flow solution for two bubbles

3.1. Method of reflections

In their paper SJ showed how to reflect the uniform stream $\Psi_U = Ur^2/I_1(\mu)$ in the bubble, by finding the perturbation stream function $\chi^*(0, \alpha)$ which must be added to Ψ_U to satisfy the boundary conditions on the bubble's surface. SJ thus found the special case for $\psi = \Psi_U$ of the linear operator $\mathcal{L}(s, \beta)$ which acts on a Stokes stream function ψ to give the perturbation caused by the spherical bubble of unit radius, centre a distance s below the origin, and cap angle β . More precisely, let ψ be the stream function of any axisymmetric Stokes flow with $\psi = 0$ on the axis and no singularities inside or on the sphere $|\mathbf{x}'| = 1$ with centre at s and radius 1. Let $\psi_{s, \beta}$ be the stream function of the flow tending to ψ at infinity past the bubble $|\mathbf{x}'| = 1$ with cap angle β , so that $\psi_{s, \beta}$ obeys the boundary conditions (12) to (15) on its surface. Then we need to find $\mathcal{L}(s, \beta)$ where

$$\mathcal{L}(s, \beta) \psi = \psi_{s, \beta} - \psi. \quad (22)$$

The operator \mathcal{I} of (10) is a special case of \mathcal{L} , as $\mathcal{I}(s, 1) = \mathcal{L}(s, 0)$, and the SJ perturbation stream function for a single bubble (see equations (9), (11)), is $\chi^*(0, \alpha) = \mathcal{L}(0, \alpha) \Psi_U$. When we have found \mathcal{L} we can use it to find the flow of an otherwise uniform stream of speed $U = 1$ past a pair of bubbles with equal radius 1, centres at 0 and s , and cap angles α, β respectively, by repeated use of the method of reflections, because

$$\begin{aligned} \Psi &= \Psi_U + \chi^*(0, \alpha) + \chi^*(s, \beta) \\ &+ \mathcal{L}(s, \beta) \chi^*(0, \alpha) + \mathcal{L}(0, \alpha) \chi^*(s, \beta) \\ &+ \mathcal{L}(0, \alpha) \mathcal{L}(s, \beta) \chi^*(0, \alpha) + \mathcal{L}(s, \beta) \mathcal{L}(0, \alpha) \chi^*(s, \beta) \\ &+ \mathcal{L}(s, \beta) \mathcal{L}(0, \alpha) \mathcal{L}(s, \beta) \chi^*(0, \alpha) + \mathcal{L}(0, \alpha) \mathcal{L}(s, \beta) \mathcal{L}(0, \alpha) \chi^*(s, \beta) \\ &+ \dots, \end{aligned} \quad (23)$$

where each line after the first gives the reflection in each bubble of the term in the line above which did not arise from a reflection in the same bubble. We may rearrange this series to give

$$\begin{aligned} \Psi &= \Psi_U + \left(\sum_{n=0}^{\infty} \{ \mathcal{L}(0, \alpha) \mathcal{L}(s, \beta) \}^n \{ \chi^*(0, \alpha) + \mathcal{L}(0, \alpha) \chi^*(s, \beta) \} \right) \\ &+ \left(\sum_{n=0}^{\infty} \{ \mathcal{L}(s, \beta) \mathcal{L}(0, \alpha) \}^n \{ \chi^*(s, \beta) + \mathcal{L}(s, \beta) \chi^*(0, \alpha) \} \right), \end{aligned} \quad (24)$$

where the first series has its singularities inside the top bubble $r = 1$, the second inside the second bubble $r' = 1$. In the next section we obtain the stream function in (24) by finding vector representations for $\chi^*(0, \alpha)$ with respect to the ϕ_k and ψ_k basis elements and similarly for $\chi^*(s, \beta)$ with respect to the ϕ'_k and ψ'_k basis elements,

finding the corresponding matrix representations for the differential operators $\mathcal{L}(0, \alpha)$ and $\mathcal{L}(s, \beta)$, and then simplifying the summations. Of course, since the bases are of finite dimension, truncation to finite dimension is required, and this requires us to investigate convergence.

3.2. *Reflection operators*

We can expand any solution Ψ to the Stokes equation which is axisymmetric, zero on the axis and whose velocity field tends to zero at infinity, as a series of functions ϕ_k and ψ_k of the form

$$\Psi = \sum_{n=1}^{\infty} (c_k \psi_k + d_k \phi_k), \tag{25}$$

which converges for sufficiently large r . For example the SJ solution for the reflection of a uniform stream in a bubble consisted of an expression of the form (25) where the vector coefficients were obtained by a solution of dual series equations of the type of (18), (19).

Using the inner product

$$\langle f, g \rangle = \int_{-1}^1 f(1, \mu) g(1, \mu) \frac{d\mu}{1-\mu^2}, \tag{26}$$

in which the integral is taken around the semicircle $r = 1, -1 < \mu < 1$, we have

$$\langle \phi_k, \phi_l \rangle = \langle \phi_k, \psi_l \rangle = \langle \psi_k, \psi_l \rangle = \frac{\delta_{kl}}{k(k+\frac{1}{2})(k+1)}, \tag{27}$$

and we can associate an infinite vector Φ with each solution of (25) as

$$\Phi = [c, d] = [(c_1, c_2, \dots), (d_1, d_2, \dots)], \tag{28}$$

where

$$c_k = \mathcal{C}_k \Psi = k(k+\frac{1}{2})(k+1) \langle \psi_k, D\Psi / (2-4k) \rangle, \tag{29}$$

$$d_k = \mathcal{D}_k \Psi = k(k+\frac{1}{2})(k+1) \langle \psi_k, \Psi - D\Psi / (2-4k) \rangle. \tag{30}$$

We also define $\mathcal{C}'_k, \mathcal{D}'_k$ by integrals corresponding to (29), (30) with ψ'_k and ϕ'_k in their integrands and with domains of integration around the semicircle $r' = 1, -1 < \mu' < 1$. It is perhaps worth mentioning that the operator D of (6) is the same in dashed coordinates. Its translation invariance is obvious if it is written in cylindrical polar coordinates.

Let $[c(\alpha), d(\alpha)]$ be the vector Φ representing the SJ solution for a bubble $r = 1$ of cap angle α moving with speed $U = 1$. Then

$$c_k(\alpha) = C_k^*, \quad d_k(\alpha) = -C_k, \tag{31}$$

as in (11) and (16), and

$$\mathcal{L}(s, \beta) \chi^*(0, \alpha) = \sum_{k=1}^{\infty} [c_k(\alpha) \mathcal{L}(s, \beta) \psi_k + d_k(\alpha) \mathcal{L}(s, \beta) \phi_k] \tag{32}$$

since from its definition \mathcal{L} is linear.

Since ψ_n and ϕ_n satisfy $D^2\psi = 0$, so do $\mathcal{L}\psi_n$ and $\mathcal{L}\phi_n$, and these functions can be expanded in series involving ψ_n and ϕ_n . Then the Φ vector representing $\mathcal{L}(s, \beta) \chi^*(0, \alpha)$ is $[c(\alpha), d(\alpha)] \Lambda(s, \beta)$, where

$$\Lambda(s, \beta) = \begin{pmatrix} A & B \\ C & D \end{pmatrix}, \tag{33}$$

is the matrix representing $\mathcal{L}(s, \beta)$, and the submatrices $\mathbf{A}, \mathbf{B}, \mathbf{C}, \mathbf{D}$ are given by

$$\begin{aligned} A_{kn} &= \mathcal{C}'_k \mathcal{L}(s, \beta) \psi_n, \\ B_{kn} &= \mathcal{D}'_k \mathcal{L}(s, \beta) \psi_n, \\ C_{kn} &= \mathcal{C}'_k \mathcal{L}(s, \beta) \phi_n, \\ D_{kn} &= \mathcal{D}'_k \mathcal{L}(s, \beta) \phi_n. \end{aligned}$$

If the two bubbles did not interact, the stream function for the flow past them could be represented by the following vector Φ_0 :

$$\Phi_0 = [c(\alpha), d(\alpha), c(\beta), d(\beta)], \tag{34}$$

where the first and second pairs of terms represent the expansion coefficient in terms of functions centred on the first and second bubbles respectively. The actual stream function for interacting bubbles is given by (24) and is represented by

$$\Phi = \Phi_0 \sum_{n=0}^{\infty} \mathbf{P}^n = \Phi_0 (\mathbf{I} - \mathbf{P})^{-1}, \quad \mathbf{P} = \begin{pmatrix} \mathbf{0} & \Lambda(s, \beta) \\ \Lambda(0, \alpha) & \mathbf{0} \end{pmatrix}, \tag{35}$$

where \mathbf{I} is the unit matrix and $\mathbf{0}$ is the matrix whose elements are all equal to 0. Thus the method of reflections will converge if the norm $\|\mathbf{P}\| < 1$. Since \mathbf{P} is of infinite order but practical computing can only be done with finite matrices we truncate all series involving ψ_k, ϕ_k to $k \leq N$. The truncation of \mathbf{P} is then of order $4N$ and its supremum norm $\|\mathbf{P}_{4N}\|$ must tend to $\|\mathbf{P}\|$ as $N \rightarrow \infty$. This question is investigated later, in §3.3.

3.3. Calculation of matrix elements

In order to find \mathbf{P} we begin with the inner products $\mathcal{C}'_k \mathcal{L} \psi_1, \mathcal{D}'_k \mathcal{L} \psi_1, \mathcal{C}'_k \mathcal{L} \phi_1, \mathcal{D}'_k \mathcal{L} \phi_1$. Consider a general Stokes stream function $\Psi_0(r, \mu)$, which is zero on the axis except at $\mathbf{x} = \mathbf{p}, |\mathbf{p}| > 1$, where its corresponding velocity field has a singularity. If Ψ is the stream function for the flow Ψ_0 as perturbed by the bubble $r = 1$ with gap angle α , the boundary conditions corresponding to those in §2 are

$$\Psi \rightarrow \Psi_0 \quad \text{as } \mathbf{x} \rightarrow \mathbf{p}, \tag{36}$$

$$\frac{\partial \Psi}{\partial r} = 0 \quad (0 \leq \theta < \alpha, \quad r = 1), \tag{37}$$

$$p_{r\theta}(\Psi) = 0 \quad (\alpha < \theta \leq \pi, \quad r = 1), \tag{38}$$

and the function Ψ can be written for $r > 1$ as

$$\Psi = \Psi'_0 + \sum_{n=1}^{\infty} [c_k \psi_k + d_k \phi_k] \tag{39}$$

where $\Psi'_0 = \Psi_0 + \mathcal{L}(0, 0) \Psi_0 = \Psi_0 + \mathcal{J}(0, 1) \Psi_0$, which would be the complete solution for $\alpha = 0$ (Harper 1983). Applying the boundary conditions, we find that $c_k = -d_k$, and c_k can be found from the dual series equations

$$\sum_{k=1}^{\infty} c_k I_k(\mu) = -\frac{1}{2} \frac{\partial \Psi'_0}{\partial r} \quad (0 \leq \theta < \alpha, \quad r = 1), \tag{40}$$

$$\sum_{k=1}^{\infty} c_k (2k+1) I_k(\mu) = \frac{1}{2} p_{r\theta}(\Psi'_0) = 0 \quad (\alpha < \theta \leq \pi, \quad r = 1). \tag{41}$$

If $\Psi_0 = \psi_1$, Harper's (1983) inversion theorem gives its reflection in a capless bubble at $r' = 1$ as

$$\mathcal{L}(s, 0) \psi_1 = -\frac{r'^2(1-\mu'^2)}{2|s|(r'^2 + 2r'\mu'/s + 1/s^2)^{\frac{3}{2}}} \tag{42}$$

so that $\Psi'_0 = \frac{1}{2}r'^2(1-\mu'^2) \left(\frac{1}{(r'^2 + 2r'\mu'/s + s^2)^{\frac{3}{2}}} - \frac{1}{|s|(r'^2 + 2r'\mu'/s + 1/s^2)^{\frac{3}{2}}} \right)$, (43)

and the dual series equations (40) and (41) are now of the form of equations (18) and (19) with $f(\theta')$ given by

$$f(\theta') = -\frac{1}{2} \frac{\partial}{\partial r'} (\Psi'_0)_{r'-1} \tag{44}$$

$$= -\frac{(1-\mu'^2)(s^2-1)}{4(s^2 + 2s\mu' + 1)^{\frac{3}{2}}}. \tag{45}$$

Clearly $f(\theta')$ satisfies the conditions required in §2 because it is non-singular on $0 \leq \theta' \leq \pi$, as $|s| > 1$. Then (21) gives

$$h(u) = -\frac{1}{4\pi} (s^2-1) \operatorname{cosec} \left(\frac{1}{2}u\right) \frac{d}{du} \int_0^u \frac{\sin^2 \theta d\theta}{(s^2 + 2s \cos \theta + 1)^{\frac{3}{2}} (\cos \theta - \cos u)^{\frac{1}{2}} (1 + \cos \theta)},$$

and on substituting $x = \cos u$ and $A = (s^2 + 1)/2s$ we obtain

$$\begin{aligned} h(u) &= -\frac{s^2-1}{4\pi|2s|^{\frac{3}{2}}} \operatorname{cosec} \left(\frac{1}{2}u\right) \frac{d}{du} \int_x^1 \frac{(1-\mu) d\mu}{(\mu-x)^{\frac{1}{2}} |\mu+A|^{\frac{3}{2}}} \\ &= -\frac{|s+1|(s^2-1) \sin u}{32^{\frac{1}{2}} \pi s^2 (A + \cos u)^2}, \end{aligned} \tag{46}$$

so that the coefficients in the dual series equations (40) and (41) are given by

$$c_k = -\frac{\operatorname{sgn}(s)(s+1)(s^2-1)}{8\pi s^2} \left(\frac{k \sin k_1 \alpha + k_1 \sin k \alpha}{A + \cos \alpha} - k k_1 \int_0^\alpha \frac{\cos k_1 u + \cos k u}{A + \cos u} du \right), \tag{47}$$

where $k_1 = k + 1$ and $|s + 1|$ has been replaced by $(s + 1) \operatorname{sgn}(s)$ since $|s| \geq 2$ in all cases. In §3.4 we obtain a convergent series for the above integral. If one interchanges the positions of the Stokeslet and the bubble, the same equation for c_k holds with s replaced by $-s$.

The matrix elements representing the reflection of the first basis element ψ_1 , i.e. the corresponding coefficients in (39), can be obtained from (47) and the definition of an inverse stream function in (10) as

$$\mathcal{L}(s, 0) \psi_1 = \frac{1}{2} \operatorname{sgn}(s) \sum_{k=1}^{\infty} (-1)^{k+1} k(k+1) \left(\frac{s^{-k}}{2k-1} \psi'_k - \frac{s^{-k-2}}{2k+3} \phi'_k \right), \tag{48}$$

which converges if $r' > |1/s|$; this includes the whole region of interest outside the bubble, where $r' > 1$, because $|s| > 2$.

The procedure can now be repeated to expand the reflection of ϕ_1 , but no new integrals need to be done. We can write

$$\Psi_0 = \phi'_1 = \frac{r'^2(1-\mu'^2)}{2(r'^2 + 2r'\mu'/s + s^2)^{\frac{3}{2}}}, \tag{49}$$

whose inverse stream function is given by

$$\mathcal{L}(s, 0) \phi'_1 = -\frac{r'^4(1-\mu'^2)}{2|s|^3(r'^2/s^2 + 2r'\mu'/s + 1)^{\frac{3}{2}}} \tag{50}$$

$$= \frac{1}{2} \operatorname{sgn}(s) \sum_{k=1}^{\infty} (-1)^k k(k+1) s^{-(k+2)} \psi'_k, \tag{51}$$

so that $f(\theta')$ can now be written as

$$f(\theta') = -\frac{1}{2} \frac{\partial}{\partial r'} (\Psi'_0)_{r'-1} \tag{52}$$

$$= \frac{1}{4}(1-\mu'^2) \left[\left(2s \frac{\partial}{\partial s} \frac{1}{(s^2 + 2s\mu' + 1)^{\frac{3}{2}}} \right) + \frac{5}{(s^2 + 2s\mu' + 1)^{\frac{3}{2}}} \right]. \tag{53}$$

This formulation allows us to use the expressions for $h(u)$ obtained in reflecting ψ_1 . Comparing the above expression for $f(\theta')$ with (45) and using the fact that \mathcal{L} and $(\partial/\partial s)$ commute, we obtain

$$c'_k = -\left[\left(2s \frac{\partial}{\partial s} \frac{c_k}{s^2 - 1} \right) + 5 \frac{c_k}{s^2 - 1} \right], \tag{54}$$

where c_k is given by (47), and the c'_k are the coefficients in equations (40) and (41) if Ψ_0 is given by (49).

3.4. Recurrence relations

Having found the reflection operators for ψ_1 and ϕ_1 , we construct them for ψ_n and ϕ_n by the usual differentiation procedure. We have

$$\psi_n = \mathcal{T}_n \psi_1 + a_n \phi_{n-2}, \tag{55}$$

$$\phi_n = \mathcal{O}_n \phi_1, \tag{56}$$

where the differential operators \mathcal{T}_n and \mathcal{O}_n are defined by

$$\mathcal{T}_n = (-1)^{n-1} (2n-1) \frac{2}{(n+1)!} \frac{\partial^{n-1}}{\partial s^{n-1}}, \tag{57}$$

$$\mathcal{O}_n = (-1)^{n-1} \frac{2}{(n+1)!} \frac{\partial^{n-1}}{\partial s^{n-1}}, \tag{58}$$

the differentiations of $\psi_1(r, \mu)$ and $\phi_1(r, \mu)$ are performed at constant r', μ' , using equations (2)–(4), and the coefficients a_n are defined by

$$a_n = \frac{(n-1)(n-2)}{n(n+1)}. \tag{59}$$

Similarly $\psi'_n = \mathcal{T}'_n \psi'_1 + a_n \phi'_{n-2}$ where $\mathcal{T}'_n(s) = \mathcal{T}_n(-s)$ except that the implied differentiations are now performed at constant r, μ , and $\phi'_n = \mathcal{O}'_n \phi'_1$ where \mathcal{O}'_n is to \mathcal{O}_n as \mathcal{T}'_n is to \mathcal{T}_n . The multipole relations (55), (56) are obviously true for $n = 1$ and can be verified for higher n by induction, using the recurrence relations for Legendre

polynomials. The matrix elements representing the reflection of the inverse stream function for each basis element are now easily obtained as

$$\mathcal{F}_n \mathcal{C}'_k \mathcal{L}(s, 0) \psi_1 = \frac{(-1)^k \operatorname{sgn}(s) k(k+1)(k+n-2)!(2n-1)}{(2k-1)(n+1)!(k-1)!s^{k+n-1}}, \tag{60}$$

$$\mathcal{F}_n \mathcal{D}'_k \mathcal{L}(s, 0) \psi_1 = \frac{(-1)^{k-1} \operatorname{sgn}(s)(k+n)!(2n-1)}{(2k+3)(n+1)!(k-1)!s^{k+n-1}}, \tag{61}$$

$$\mathcal{O}_n \mathcal{C}'_k \mathcal{L}(s, 0) \phi_1 = \frac{(-1)^k \operatorname{sgn}(s)(k+n)!(2n-1)}{(n+1)!(k-1)!s^{k+n+1}}, \tag{62}$$

$$\mathcal{O}_n \mathcal{D}'_k \mathcal{L}(s, 0) \phi_1 = 0. \tag{63}$$

To calculate the coefficients of the dual series equations for reflections of higher-order basis elements we need recurrence relations, which will now be given. Applying the operators \mathcal{F}_n and \mathcal{O}_n to the integrals for c_k given in (47), we find that if $k_1 = k + 1$ as before,

$$\mathcal{F}_n c_k = -\frac{1}{8\pi} \operatorname{sgn}(s) \left[t_n(\alpha) (k \sin k_1 \alpha + k_1 \sin k \alpha) - k k_1 \int_0^\alpha t_n(u) (\cos k_1 u + \cos k u) du \right], \tag{64}$$

and a similar equation with o_n, \mathcal{O}_n replacing t_n, \mathcal{F}_n , where

$$t_n(u) = \frac{8(2n-1)}{n(n+1)} \operatorname{Re} \frac{1 - e^{-iu}}{(s + e^{-iu})^n}, \tag{65}$$

and
$$o_n(u) = \frac{8}{n(n+1)} \operatorname{Re} \left[\frac{1}{1 + e^{-iu}} \left(\frac{3}{(s + e^{-iu})^n} + \frac{2n e^{-iu}}{(s + e^{-iu})^{n+1}} \right) \right]. \tag{66}$$

The functions t_n and o_n behave regularly, since $|s| > 2$ and the apparent singularity in the integrand of $\mathcal{O}_n c_k$ at $u = \pi$ is actually removable.

In order to compute the integral in (64), we define

$$f(k, n) = \operatorname{Re} \int_0^\alpha \frac{e^{iuk} du}{(s + e^{-iu})^n}, \tag{67}$$

with k and n integers. The following recurrence relations are easily confirmed:

$$f(k, n) = \frac{1}{k} \operatorname{Im} \frac{e^{iak}}{(s + e^{-i\alpha})^n} - \frac{n}{k} f(k-1, n+1), \tag{68}$$

$$f(k, n) = \frac{1}{s} (f(k, n-1) - f(k-1, n)), \tag{69}$$

from which we can prove that

$$f(k, n) = \frac{1}{sk} \left[\operatorname{Im} \frac{e^{iak}}{(s + e^{-i\alpha})^{n-1}} - (n+k-1) f(k-1, n) \right]. \tag{70}$$

The function $f(k, n)$ can be evaluated for all integers k and all positive integers n by using these recurrence relations with the values of $f(-1, n)$ and $f(0, 1)$ given by the following expressions:

$$f(-1, n) = \frac{1}{n-1} \operatorname{Im} \frac{1}{(s + e^{-i\alpha})^{n-1}}$$

$$f(0, 1) = \frac{\alpha}{s} - \frac{1}{s} \tan^{-1} \left(\frac{\sin \alpha}{s + \cos \alpha} \right). \tag{71}$$

The best sequence to reduce accumulated error in numerical work is to compute $f(k, 1)$ for negative k using (70) and then compute the other terms with (68).

The integrals in (64) can now be expressed in terms of $f(k, n)$ as

$$\int_0^\infty t_n(u) (\cos k_1 u + \cos ku) du = \frac{4(2n-1)}{n(n+1)} [f(k_1, n) - f(k-1, n) + f(-k, n) + f(-k-2, n)], \quad (72)$$

similarly

$$\int_0^\infty o_n(u) (\cos k_1 u + \cos ku) du = -\frac{12}{n(n+1)} [f(k_1, n) - f(k-1, n)] - \frac{8}{n+1} [f(k, n+1) + f(-k_1, n+1)]. \quad (73)$$

The above completes the solution for the case of two capped bubbles. It is now necessary to investigate the convergence of the series.

3.5. Investigating convergence

Since $|\psi_n|, |\phi_n|, |\psi'_n|, |\phi'_n|$ are all smaller than $n^{-\frac{1}{2}}$ on and outside the bubbles $r = 1, r' = 1$, by a theorem of Stieltjes (Sansone 1959, pp. 199–200), the series for Ψ converge absolutely and uniformly if the supremum norm $\|\Phi\|$, which is the modulus of the numerically largest element of Φ , exists. From (35)

$$\|\Phi\| \leq \|\Phi_0\| \sum_{n=0}^\infty \|\mathbf{P}\|^n = \frac{\|\Phi_0\|}{1 - \|\mathbf{P}\|}, \quad (74)$$

if $\|\mathbf{P}\| < 1$. From (16), (31) and (34), $\|\Phi_0\| < \frac{3}{2} + 7/12\pi = 1.6857$ to five figures.

Thus the supremum norm of the solution vector exists if $\|\mathbf{P}_N\|$ has a finite limit $\|\mathbf{P}\|$ as $N \rightarrow \infty$, and $\|\mathbf{P}\| < 1$. The former depends on the convergence of coefficients of the expansion in (39).

Using (67) and (68) we obtain the asymptotic behaviour of the intermediate function $f(k, n)$ as

$$|f(k, n)| \leq \frac{1}{|k|} d^{-n} \left(1 + \frac{n\pi}{d}\right) \sim \frac{n\pi}{|k|} d^{-n-1} \quad (n \gg d), \quad (75)$$

where $d = |s| - 1$. Then from (64) we obtain to leading order in n and k

$$|\mathcal{F}_n c_k| \sim 8nd^{-n-1} \quad (n \gg d). \quad (76)$$

The above determines the rate of convergence of the terms dependent on the cap angle. In the stream function expansion these terms have added to them the expansion of the inverse stream function, whose asymptotic expansion we must add to (76) to determine the asymptotic behaviour of the stream function.

We find, using (60)–(63), that

$$\mathcal{C}'_k \mathcal{L}(s, 0) \psi_n \sim K|s|^{-n-1}, \quad (77)$$

$$\mathcal{D}'_k \mathcal{L}(s, 0) \psi_n \sim K|s|^{-n-1}, \quad (78)$$

$$\mathcal{C}'_k \mathcal{L}(s, 0) \phi_n \sim K(n+3)(n+2)|s|^{-n-4}, \quad (79)$$

where K is a constant independent of n .

As can be seen from (35), $\|\mathbf{P}\| = \|\mathbf{\Lambda}(s, \alpha)\|$, where α is the cap angle of one of the two bubbles. The norm of $\mathbf{\Lambda}$ can in turn be written as

$$\|\mathbf{\Lambda}(s, \alpha)\| = \max_{k, n} (|A_{kn}|, |B_{kn}|, |C_{kn}|, |D_{kn}|).$$

We see from (39) that the series for $\|\mathbf{P}\|$ converges as least as fast as the series $\sum K[16nd^{-n-1} + |s|^{n+1} + (n+3)(n+2)|s|^{-n-4}]$. If $|s| > 2.4$ then an accuracy of 1% in $\|\mathbf{P}\|$ requires $N \sim 10$, and \mathbf{P} is then truncated to order $4N$.

The actual value to which $\|\mathbf{P}_{4N}\|$ converges as $N \rightarrow \infty$ has unfortunately not been found analytically; all that has been determined is how the series for the norm of \mathbf{P}_{4N} converges. Numerical calculations not reported in detail here have shown that the norm of \mathbf{P}_{4N} and its limit for large N are indeed less than one in all cases where $|s| > 2$. This ensures that drag coefficients will be accurately found from modest values of N , but unfortunately calculating Ψ is more demanding. This is because the arguments based on the supremum norm limit the absolute error in Ψ , but near a bubble surface (and especially near a stagnation point) Ψ is very small, and a streamline plot needs small relative error.

3.6. Extensions of the problem

The problem above could be extended, without the need for much further calculation, to the case of many bubbles with different cap sizes rising in a line, or to one or more bubbles rising beneath a plane surface. Thus for the case of three bubbles with cap angles α , β and γ and centres at $\mathbf{x} = \mathbf{0}$, $\mathbf{x} = s_1 \mathbf{k}$, $\mathbf{x} = s_2 \mathbf{k}$ respectively, the reflection matrix becomes

$$\mathbf{P} = \begin{pmatrix} \mathbf{\Lambda}(0, \alpha) & \mathbf{0} & \mathbf{\Lambda}(s_2, \gamma) \\ \mathbf{0} & \mathbf{\Lambda}(s_1, \beta) & \mathbf{\Lambda}(s_2, \gamma) \\ \mathbf{\Lambda}(0, \alpha) & \mathbf{\Lambda}(s_1, \beta) & \mathbf{0} \end{pmatrix}, \quad (80)$$

and the initial SJ vector is given by

$$\Phi_0 = [c(\alpha), d(\alpha), c(\beta), d(\beta), c(\gamma), d(\gamma)]. \quad (81)$$

In the case of a bubble with its centre at $r = s$ rising beneath a plane free surface $\theta = \frac{1}{2}\pi$, the reflection matrix is given by

$$\mathbf{P} = \mathbf{\Lambda}(s, \alpha) \mathbf{R}, \quad (82)$$

where \mathbf{R} is the representation of the operator \mathcal{R} reflecting a general stream function in a plane surface, i.e. $(\mathcal{R}\psi)(r, \mu) = -\psi(r, -\mu)$, whose matrix elements are given by

$$\begin{aligned} R_{kl} &= (-1)^k \delta_{kl} & (1 \leq k \leq N), \\ R_{kl} &= (-1)^{k+N} \delta_{kl} & (N < k \leq 2N). \end{aligned}$$

4. Convective diffusion

4.1. The first bubble

So far we have found flow patterns and drag coefficients for given cap sizes without worrying about whether the configuration could arise naturally in a surfactant solution. But both bubbles are rising in the same liquid, and the second bubble rises in the wake of the first. The consequences of this will now be explored.

SJ showed that stagnant caps occur in two important situations: strong barriers to absorption and desorption, and high Péclet number for a soluble surfactant. We treat only the latter case, extending the theory of Harper (1973) as required for two bubbles.

Let Π be the surface pressure, i.e. the difference $\sigma_p - \sigma$ between the surface tensions σ_p of pure solute and σ of the actual solution. In equilibrium

$$\Pi = R_g T h c \tag{83}$$

in an ideal solution, where R_g is the gas constant, T is the absolute temperature, h is the adsorption depth, a constant characterizing the surfactant, and c is the concentration of surfactant in the bulk fluid. At all points in the bulk fluid, whether on the surface or not, it is convenient to define Π by (83) and work in terms of it instead of c . The convective diffusion equation for steady flow can thus be written

$$\mathbf{u} \cdot \nabla \Pi = \kappa \nabla^2 \Pi, \tag{84}$$

where κ is the diffusivity of the surfactant. Let the bubble's Péclet number $Pe = 2Ua/\kappa \gg 1$, where a is the radius. (The preceding Stokes flow theory was easier with coordinates scaled so that $a = 1$, but now it is better for physical dimensions to be included explicitly.) Diffusion will be significant only in a thin layer around the bubble, and (84) reduces on the free part of the surface to

$$\frac{1}{a^3 u_\theta \sin^2 \theta} \frac{\partial \Pi}{\partial \theta} = \kappa \frac{\partial^2 \Pi}{\partial \Psi^2}. \tag{85}$$

If
$$x = \int_\pi^\theta u_\theta \sin^2 \theta \, d\theta,$$

so that $x = 0$ at the top stagnation point, $x = x^* > 0$ at the cap edge, and

$$y = \frac{1}{2}(\kappa a^3)^{-\frac{1}{2}} \Psi,$$

we find that a good approximation on the free part of the bubble is

$$4 \frac{\partial \Pi}{\partial x} = \frac{\partial^2 \Pi}{\partial y^2}, \tag{86}$$

and so
$$\Pi = \Pi_\infty \operatorname{erf}(yx^{-\frac{1}{2}}), \tag{87}$$

which at the edge of the cap is

$$\Pi = \Pi_\infty \operatorname{erf}[(Pe U/8x^*)^{\frac{1}{2}}(\Psi/Ua^2)]. \tag{88}$$

Here Π_∞ is the equilibrium surface pressure of the solution far from the bubbles. Note that θ in this paper is the same as in SJ but is $(\pi - \theta)$ in the notation of Harper (1973).

On the first bubble's cap $u_\theta = 0$ approximately. Let $\Pi = \Pi^*$ at the rear stagnation point, and $\Pi = \Pi_c(\theta)$ at any position on the cap. Then the rate of strain $-E$ on the cap is a function of θ which can be calculated from the purely viscous theory of previous sections and is connected to the variation of Π through the boundary condition on surface shear stress

$$\frac{d\Pi_c(\theta)}{d\theta} = \eta a E. \tag{89}$$

Close to the cap the diffusion boundary-layer equation (84) simplifies (Lighthill 1950; Harper 1973) to

$$9 \frac{\partial \Pi}{\partial X} = \frac{1}{Y} \frac{\partial^2 \Pi}{\partial Y^2}, \tag{90}$$

where $\Psi = Y^2$ and

$$X = \int_{\theta}^{\alpha} 9\kappa(Ea^5 \sin^3 \theta)^{\frac{1}{2}} d\theta > 0$$

on the cap. Let $X = X^*$ at the rear stagnation point. As $\Pi \gg \Pi_{\infty}$ on the cap (Harper 1973), the solution of (90) throughout the diffusion boundary layer on the cap can be given in terms of the surface distribution $\Pi_c(\theta)$ of Π as

$$\Pi = \int_0^X G'(t) H(Y\{X-t\}^{-\frac{1}{2}}) dt, \quad (91)$$

where $G(X) = \Pi_c(\theta)$ and

$$H(z) = \frac{\int_z^{\infty} \exp(-v^3) dv}{\int_0^{\infty} \exp(-v^3) dv} = \frac{\int_z^{\infty} \exp(-v^3) dv}{\Gamma(\frac{4}{3})}. \quad (92)$$

The function H is of course the analogue for (90) of the error-function solution of (86).

In steady flow the total mass flux of surfactant to the bubble surface vanishes. This condition gives $\int_0^{\pi} (\partial\Pi/\partial r) \sin \theta d\theta = 0$, (Harper (1973), where $\partial\Pi/\partial r$ is evaluated at the surface, i.e.

$$2\Pi_{\infty} \left(\frac{x^*}{\pi\kappa a} \right)^{\frac{1}{2}} = \frac{1}{6\sqrt{2a^2\kappa}\Gamma(\frac{4}{3})} \int_0^{X^*} (X^* - X)^{\frac{1}{2}} g'(X) dX; \quad (93)$$

the left-hand side of (93) comes from the free part of the surface and the right-hand side from the stagnant cap.

For a very small cap ($\alpha \ll 1$) on an isolated bubble, $u_{\theta} = -\frac{1}{2}U \sin \theta$ on the free part, $x^* = \frac{2}{3}U$, $E = (4U\theta/\pi a)(\alpha^2 - \theta^2)^{-\frac{1}{2}}$ on the cap, and $\Pi^* = 4U\eta\alpha/\pi$ approximately (Harper 1973), and (93) implies that

$$\alpha = 0.99954(\Pi_{\infty}/U\eta)^{\frac{1}{2}}(Ua/\kappa)^{\frac{1}{3}}, \quad (94)$$

$$\Pi^*/\Pi_{\infty} = 3.9981(U\eta/\Pi_{\infty})^{\frac{1}{2}}(Ua/\kappa)^{\frac{1}{3}} = 3.9951(Ua/\kappa)^{\frac{1}{2}}\alpha^{-\frac{1}{2}}. \quad (95)$$

These equations are correct to order of magnitude even if α is not small; the last part of (95) confirms that Π^* is much larger than Π_{∞} , by a factor of order $Pe^{\frac{1}{2}}$. The numerical factors in (95) differ from those in Harper (1973) because he inadvertently used $(X^*)^{\frac{1}{2}}$ instead of the correct $(X^* - X)^{\frac{1}{2}}$ in his analogue of (95). Equation (3.3) of that paper also contained a minor typographical error, $\psi = \frac{1}{2}Em'^2s'^2$ instead of the correct $\psi = \frac{1}{2}Em's'^2$ on the cap. In the present notation this is $\Psi = \frac{1}{2}Ea(r-a)^2 \sin \theta$.

4.2. The diffusion wake and the second bubble

As in Harper (1974), diffusion in the stagnation regions and the wake between two bubbles will be negligible provided that their distance apart is much smaller than $Pe^{\frac{1}{2}}a$, a condition that is easily satisfied if Pe is large. It follows that convective diffusion begins on the second bubble from the same surfactant distribution $\Pi(\Psi)$ that it ended with on the first bubble. Furthermore, according to (87), the free part of the surface makes Π significantly different from Π_{∞} in a region $\Psi/Ud^2 = O(Pe^{-\frac{1}{2}})$, while the cap makes it vary by the much larger amount $O(\Pi_{\infty}Pe^{\frac{1}{2}})$ in the much smaller region $\Psi/Ua^2 = O(Pe^{-\frac{1}{2}}Pe^{-\frac{1}{2}})$. This is easy to see physically from the condition that in steady flow the surfactant flux in the wake behind a bubble must

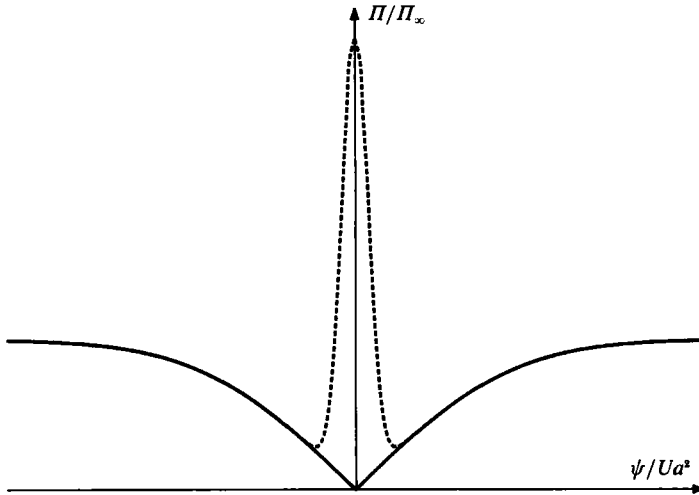


FIGURE 1. Schematic variation of surface pressure with stream function across the wake of a bubble.

be the same as that in front of it, i.e. that $\int_0^\infty (\Pi - \Pi_\infty) d\Psi$ be unchanged. In the graph of surfactant distribution shown in figure 1, the error function profile is modified by a high narrow 'spike' on the wake centreline such that the total area is unchanged by the bubble.

One effect of such a surfactant distribution is to stabilize a line of bubbles to small sideways displacements (Harper 1970). If a bubble below the first is slightly displaced, say to the left, its right-hand side will encounter more contaminated liquid of lower surface tension. Stresses will then appear around the bubble's surface moving liquid from right to left, and so the bubble itself will be propelled from left to right. Note that this effect will occur only for sideways displacement d small enough to keep the streamline through that bubble's top stagnation point in the 'spike', i.e. $\Psi = O(Ua^2 Pe^{-\frac{1}{2}})$, or $d = O(a Pe^{-\frac{1}{2}})$. For larger displacements than that, up to $d = O(a Pe^{-1})$, the lower bubble will be in the region where Π increases away from the wake centreline, and an imposed displacement will tend to increase. The vertical configuration is therefore stable to very small sideways displacements but unstable to larger ones.

A second effect (reported here for the first time) is that the first bubble brings the surfactant towards the wake centreline, so that the second bubble behaves as if rising in more contaminated fluid, with a larger stagnant cap, and it rises slower than the first. We now show this for the simplest special cases that reveal the phenomenon: two bubbles many radii apart, or closer together but with small stagnant caps. Because $Pe \gg 1$, the diffusion flux of surfactant onto the free part of the second bubble is just $(x_2^* + x^*)^{\frac{1}{2}}/x^{*\frac{1}{2}}$ times the flux onto the free part of the first, where

$$x_2^* = \int_\pi^{\alpha_2} u_\theta \sin^2 \theta d\theta, \tag{96}$$

the equivalent for the second bubble of x^* for the first. Physically, the surfactant spike diffuses almost immediately onto the second bubble, and the error-function distribution then continues to broaden gradually on the second bubble from where it left off on the first.

If the bubbles are far apart or the caps are small, $x^* = x_2^*$ approximately, and the surfactant flux onto the second bubble's free part is $\sqrt{2}$ times that onto the first. Diffusion off the second bubble's cap is found in the same way as for the first, and so

$$\left(\frac{x^* + x_2^*}{x^*}\right)^{\frac{1}{2}} = \frac{\int_0^{X_2^*} (X_2^* - X)^{\frac{3}{2}} g'_2(X) dX}{\int_0^{X^*} (X^* - X)^{\frac{3}{2}} g'(X) dX}, \quad (97)$$

where g_2, X_2^* are the values of g, X^* on the second bubble. Equation (97) shows that the second bubble rises more slowly, and the two bubbles will gradually separate.

If, however, there are three or more bubbles in the line, purely viscous interactions show that the second rises faster than the first if the surfaces are either completely clogged (Gluckman, Pfeffer & Weinbaum 1971; Pruppacher & Klett 1978, p. 636) or completely free (Harper 1983), and these interactions decay to zero inversely as the distance apart. Viscous interactions between stagnant-cap bubbles have the same properties, but the details will not be reported here.

The surfactant-induced interaction is different: it does not decay with separation until s is large, of order $Pe^{\frac{1}{2}}$, and its tendency is to make the lower bubbles more contaminated, rise slower, and so spread the line out vertically.

5. Conditions for validity

5.1. General

The foregoing analysis contains a number of assumptions which must all be satisfied if it is to apply to real bubbles in a real fluid. First, the Reynolds and Péclet numbers must obey

$$Re = 2Ua/\nu \ll 1, \quad (98)$$

$$Pe = 2Ua/\kappa \gg 1. \quad (99)$$

In water, typical surfactants have κ of order $\nu/2000$, and so a bubble of the right size to have $Re = 0.1$ will have Pe near 200 which is hardly large enough. However, the situation is better in more viscous liquids, because the Sutherland–Einstein law of diffusion (see, for example, Pais 1982, pp. 91–92) makes $\nu\kappa$ nearly constant, and Pe will then be larger for the same Re . Secondly, variations in surface tension must be much smaller than its mean value for the surfactant solution to be ideal. The condition is most stringent at rear stagnation points, where it requires

$$\Pi_{\infty} Pe^{\frac{1}{2}} \ll \sigma_p. \quad (100)$$

Thirdly, for the shape to be close to spherical it is also necessary that viscous stresses be much smaller than the excess pressure inside bubbles due to surface tension, i.e.

$$U\eta/\sigma_p \ll 1. \quad (101)$$

In addition to these conditions, there is another more subtle one which arises from the surfactant spike's effects on the front stagnation region of the second bubble. The extra surfactant in the spike will diffuse quickly onto this region, reduce the surface tension there and speed up the flow locally, as it did in the numerical work of LeVan & Holbrook (1989) when they calculated the effect on a single rising drop at moderate Re of a surfactant soluble in the dispersed phase. We need the condition that the flow be speeded up only slightly.

5.2. The second bubble's front stagnation region

Locally we may analyse an axisymmetric stagnation region using cylindrical polar coordinates (ϖ, z) , where ϖ is the distance from the axis of symmetry and z measures distance parallel to the axis from the stagnation point. Payne & Pell (1960) gave the linearly independent solutions of the Stokes flow equations as $\varpi^2 z \Psi_3$, $\varpi^2 \Psi_3$, where Ψ_3 is the general solution of

$$\frac{\partial^2 \Psi_3}{\partial \varpi^2} + \frac{3}{\varpi} \frac{\partial \Psi_3}{\partial \varpi} + \frac{\partial^2 \Psi_3}{\partial z^2} = 0. \tag{102}$$

Now the stream function must obey the boundary conditions $\Psi \sim E\varpi^2 z$ at a great distance, where the rate of strain E can be assumed constant in this local analysis, and $\Psi = 0$ on $\varpi = 0$ and $z = 0$. Separation of variables then reveals that Ψ can be written as

$$\Psi = E\varpi^2 z \left\{ 1 + \int_0^\infty \varpi^{-1} A(\lambda) e^{-\lambda z} J_1(\lambda \varpi) d\lambda \right\}, \tag{103}$$

where J_1 is a Bessel function; on the plane $z = 0$ this gives the tangential velocity u_ϖ and shear stress τ as

$$u_\varpi = E\varpi \left\{ 1 + \int_0^\infty \varpi^{-1} A(\lambda) J_1(\lambda \varpi) d\lambda \right\}, \tag{104}$$

$$\tau = -2E\eta \int_0^\infty A(\lambda) J_1(\lambda \varpi) d\lambda. \tag{105}$$

From (105), the dynamical surface condition balancing shear stress and surface tension gradient gives the surface pressure on $z = 0$ as

$$\Pi = c_1 + 2E\eta \int_0^\infty A(\lambda) J_0(\lambda \varpi) d\lambda, \tag{106}$$

where c_1 is a constant of integration.

Upstream, in the spike, we have

$$\Pi = \Pi_\infty Pe^{\frac{1}{2}} F(\Psi Pe^{\frac{3}{2}} / Ua^2), \tag{107}$$

where F is a dimensionless function which is of order unity when its dimensionless argument is also of order unity, and which decays to zero at infinity. Convective diffusion near the second front stagnation point is given by (86), i.e. $4 \partial \Pi / \partial x = \partial^2 \Pi / \partial y^2$, where we have locally that

$$\begin{aligned} x &= a^{-3} \int_0^\infty \varpi^2 u_\varpi d\varpi \\ &= \frac{1}{4} E a^{-3} \varpi^4 \left\{ 1 + 4\varpi^{-2} \int_0^\infty \lambda^{-1} A(\lambda) J_2(\lambda \varpi) d\lambda \right\}, \end{aligned} \tag{108}$$

$$y = \frac{1}{2} (ka^3)^{-\frac{1}{2}} \Psi. \tag{109}$$

The boundary-value problem embodied in (86), (103) and (106)–(109) is completed by the condition for conservation of mass of surfactant, which is

$$\kappa \varpi \frac{\partial \Pi}{\partial z} = h \frac{\partial}{\partial \varpi} (\Pi \varpi u_\varpi), \tag{110}$$

or

$$\frac{\partial \Pi}{\partial y} = \frac{2h}{\kappa^{\frac{1}{2}} a^{\frac{3}{2}}} \frac{\partial}{\partial x} (\Pi \varpi u_w), \quad (111)$$

where the left-hand side of (110) is $R_g Th$ times the diffusion flux to the surface and the right-hand side is $R_g Th$ times the surface divergence of the surface flux of surfactant (Levich 1962; Harper 1972). This boundary-value problem is nonlinear because Ψ , x , y , Π and u_w all depend on the unknown function $A(\lambda)$, but we need not solve it in general: we only need the condition that the integral in (104) be small compared with 1. Equation (110) shows that that happens if h is sufficiently large, and we now show that $h \gg a(\Pi_\infty/U\eta)Pe^{-\frac{1}{2}}$ is large enough.

We can estimate the left-hand side of (111) by putting $\Pi = 0$ instead of using (106) as the surface boundary condition for (86). The upstream boundary condition (107) is expressible in terms of y as

$$\Pi = \Pi_\infty Pe^{\frac{1}{2}} F(2\sqrt{2}Pe^{\frac{1}{2}}U^{-\frac{1}{2}}y), \quad (112)$$

on $x = 0$, and (111) gives

$$\Pi \varpi u_w = \frac{2\kappa^{\frac{1}{2}} a^{\frac{3}{2}} \Pi_\infty Pe^{\frac{1}{2}}}{h} \int_0^\infty F(2\sqrt{2}Re^{\frac{1}{2}}U^{-\frac{1}{2}}y) \operatorname{erfc}(yx^{-\frac{1}{2}}) dy \quad (113)$$

on the surface $y = 0$ after some straightforward calculations with the standard Green function (Carslaw & Jaeger 1959, §2.4). Now ϖu_w and $x^{\frac{1}{2}}$ are both proportional to ϖ^2 , and the error function in (113) decays much faster than the F term if $x \ll UPe^{-\frac{1}{2}}$ or $\varpi \ll aPe^{-\frac{1}{2}}$, and so $\Pi = O(\Pi_\infty Pe^{-\frac{1}{2}}a/h)$ there, while if $\varpi \gg aPe^{-\frac{1}{2}}$ the error function decays more slowly, and $\Pi = O(\Pi_\infty Pe^{-\frac{1}{2}}a^3/h\varpi^2)$. To assess the importance of this distribution of surface pressure we use an approximate form which has the correct asymptotic limits, is correct to order of magnitude elsewhere, and for which all the integrals involving Bessel functions are readily available (Bateman Manuscript Project 1954), namely

$$\Pi = \frac{c_2 \Pi_\infty Pe^{-\frac{1}{2}}a/h}{1 + \varpi^2/c_3^2}, \quad (114)$$

where c_2 is a constant of order 1 and c_3 a constant of order $aPe^{-\frac{1}{2}}$. Then (106) gives

$$A(\lambda) = \frac{c_2 c_3^2 \Pi_\infty Pe^{-\frac{1}{2}}a}{2E\eta h} \lambda K_0(c_3 \lambda), \quad (115)$$

$$\begin{aligned} u_w &= E\varpi \left\{ 1 + \frac{\pi c_2 \Pi_\infty Pe^{-\frac{1}{2}}a}{8c_3 E\eta h} {}_2F_1\left(\frac{3}{2}, \frac{3}{2}; 2; -\frac{\varpi^2}{c_3^2}\right) \right\} \\ &= E\varpi \left\{ 1 + \frac{c_2 \Pi_\infty Pe^{-\frac{1}{2}}a}{9c_3 E\eta h} \int_0^{\frac{1}{2}\pi} \frac{\sin^2 t dt}{[1 + (\varpi^2/c_3^2) \sin^2 t]^{\frac{3}{2}}} \right\}. \end{aligned} \quad (116)$$

From this one can see that u_w will always be close to its value $E\varpi$ found by ignoring the surfactant spike if $\Pi Pe^{-\frac{1}{2}}a \ll E\eta hc_3$, i.e.

$$h/a \gg (\Pi_\infty/U\eta)Pe^{-\frac{1}{2}}. \quad (117)$$

5.3. A numerical example

We now give an example to show that all the simplifying assumptions can indeed hold for the same bubbles. Consider two bubbles of radius $a = 0.2$ mm rising in a liquid with the same density as water, half the surface tension, so that $\sigma_p =$

36 nM m^{-1} , 1000 times the viscosity at room temperature, so that $\nu = 10^{-3} \text{ m}^2 \text{ s}^{-1}$, and the surfactant diffusivity $\kappa = 5 \times 10^{-13} \text{ m}^2 \text{ s}^{-1}$, in agreement with the Sutherland–Einstein law. Liquids with properties such as these include castor oil and concentrated solutions of sugar or glycerin.

At low Reynolds numbers U is of order $ga^2/3\nu = 1.3 \text{ mm s}^{-1}$, the Hadamard–Rybczynski value for one bubble with no cap. In fact U is always between two thirds of that value (bubbles widely separated, 180° caps) and $1/\ln 2 = 1.443$ times it (bubbles almost touching, 0° caps; see Harper 1983). The Reynolds number Re is thus near 5×10^{-5} , the Péclet number Pe is near 10^5 , and $U\eta/\sigma_p = U\rho\nu/\sigma_p = 4 \times 10^{-3}$, which obeys (101). The work described in this paper is interesting if $U\eta/\Pi_\infty$ is of order $Re^{\frac{1}{2}}$, (see (94)), so that cap angles will be near neither 0° nor 180° . This gives Π_∞ of order 0.02 mN m^{-1} , which satisfies (100) and requires a very dilute surfactant solution. Equation (117) then requires $h \gg 2 \mu\text{m}$, i.e. the surfactant must be much more strongly adsorbed in the liquid (which in practice means less soluble) than soap or ordinary detergents are in water.

6. Results and discussion

The method presented in §3 works for the entire region where the assumptions in our boundary value problem might have been expected to apply. The stream function expansion coefficients can be calculated to 5 significant figures if $s > 2.1$ with the maximum dimension required being $N = 20$. If $s < 3.57$, of course, the caps must be sufficiently small or the eddies between the bubbles will require the boundary conditions to be more elaborate than those we used.

The forces calculated for two bubbles agreed with those of a quite independent method (Lerner 1985) of writing the boundary-value problem in bispherical coordinates (Wacholder & Weihs 1972), and using Collin's (1961) general method to find the coefficients. It thus seems that the results can be treated with confidence. The method presented in detail here worked faster for the drag coefficient and is the only one that would apply for more than two bubbles. The method using bispherical coordinates needed fewer terms to give a good streamline plot and is the only one that would easily apply to a pair of drops whose interior viscosity was too large to neglect. Both methods unfortunately demand excessive computing time to find the velocity or shear stress on a bubble surface, and we are not yet able to present numerical results for these.

The drag force on each bubble is easily calculated with the aid of Payne & Pell (1960). They showed that it depends only on the term in the stream function expansion (25) which varies as r at infinity. In our notation their result for the drag force F is

$$F = -4\pi U\eta a c_1. \quad (118)$$

Since the bubbles are the same size the buoyancy force F_B balancing the drag is

$$F_B = \frac{4}{3}\pi a^3 g \Delta\rho, \quad (119)$$

where $\Delta\rho$ is the density difference between the phases inside and outside the bubbles, and is close to ρ . In the case of the motion of two capless bubbles, or two bubbles with 180° caps, the forces experienced by each bubble are equal, by symmetry. The symmetry is destroyed by introducing caps.

If the flow is to be truly steady, the separation of the bubbles must not change, so that their velocities must be equal. This condition constrains the cap angles. We

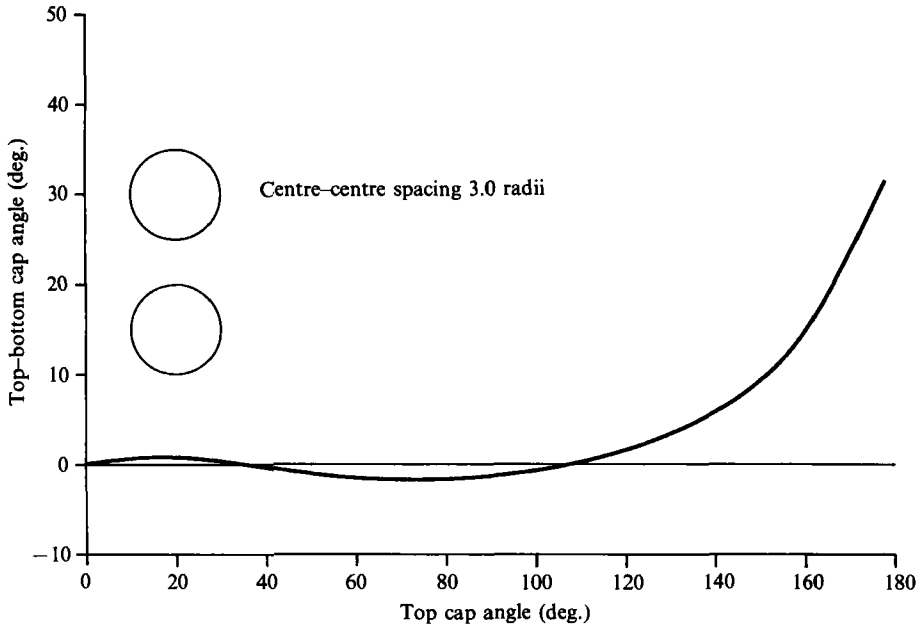


FIGURE 2. Difference between cap angles for equal drag, as a function of cap angle on the upper bubble, for $s = 3$.

must find the cap angle on one bubble, given that on the other, so that the drag forces are equal, and the separation between the bubbles does not change with time. Even if it does, the motion may still be quasi-steady, in the sense that the timescale for the bubble configuration to alter significantly is much longer than the time for vorticity to diffuse from one bubble to the other. If so the time-independent Stokes flow theory still gives a good approximation to the actual flow.

For two bubbles we calculated the equal-drag condition as follows: fix the bubble spacing s and the cap angle α of the upper bubble, evaluate the difference between the drag forces as a function of β , the cap angle of the lower bubble, and solve for the β giving zero drag difference, using Muller's method (see, for example, Nonweiler 1984, p. 171) if $\alpha \leq 150^\circ$, and the slower method of bisection for $150^\circ < \alpha < 180^\circ$, where Muller's method would not converge reliably.

The results are shown in figure 2 for $s = 3$ and in figure 3 for $s = 4$. For all separations s it turns out that the upper bubble has a larger cap for small cap angles, up to about 30° . For smaller separations the difference is larger, owing to greater interaction of the bubbles. This result can be qualitatively explained by noting that for very small caps the upper bubble's cap is in a slower flow than the lower bubble's cap, owing to the sheltering effect of the nearby lower bubble (see figure 4*a*). The upper bubble thus needs to have a larger cap in order to have the same force as the lower bubble. However, for cap angles between 30° and 110° , approximately, the lower bubble has the larger cap size. This can also be qualitatively explained by noting that for these larger cap sizes the cap on the upper bubble shelters the lower bubble from the flow more effectively than the free surface of the lower bubble shelters the upper bubble, (see figure 4*b*), and so the lower bubble must have a larger cap. Equivalently, note that the Stokes flow pattern of a uniform stream past an isolated bubble is symmetrical about the equatorial plane for only $\alpha = 0^\circ$ or $\alpha = 180^\circ$, but in any other case the disturbance to the stream is greater below the bubble

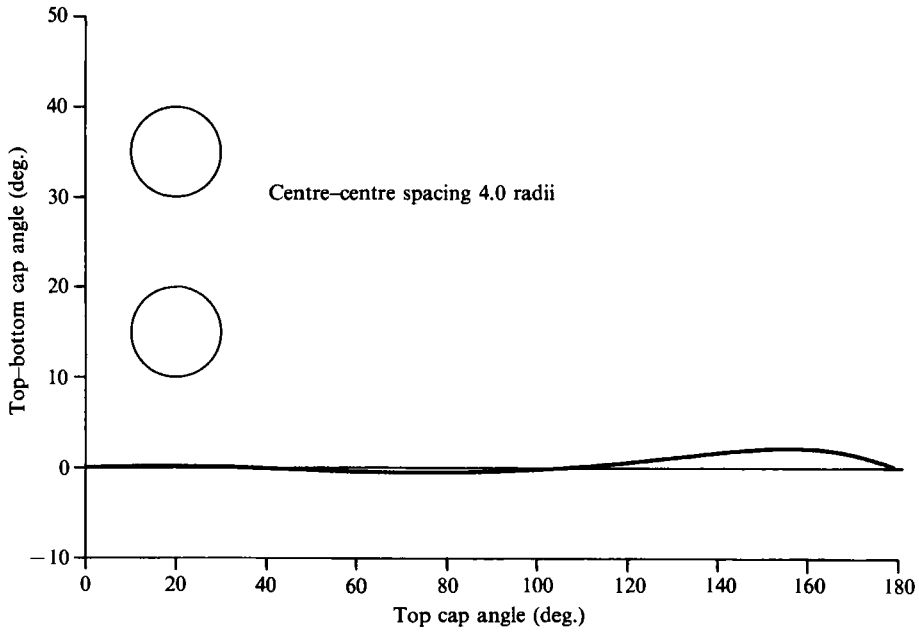


FIGURE 3. Difference between cap angles for equal drag, as a function of cap angle on the upper bubble, for $s = 4$.

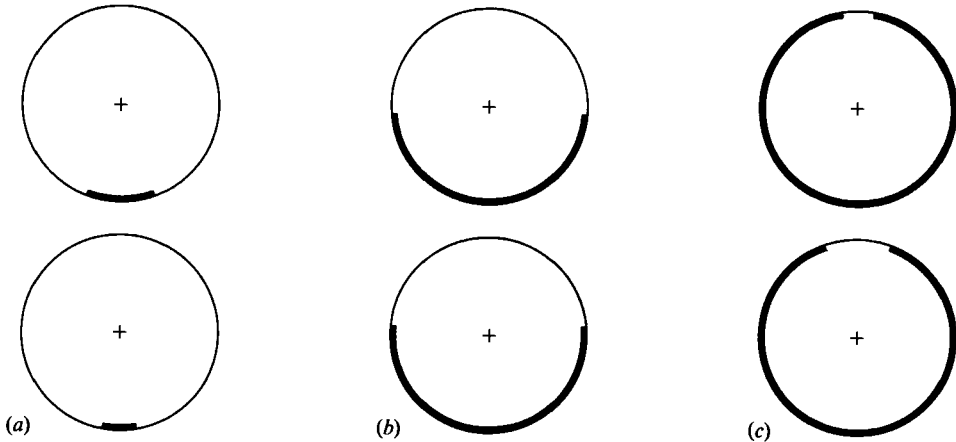


FIGURE 4. Schematic indication of different cap sizes for equal drag on each bubble, for (a) small, (b) moderate and (c) large caps.

than above it. (One might then ask why this argument does not hold for all cap sizes: the answer is that each bubble is not really in a uniform stream, but in the stream perturbed by the other bubble.)

Beyond about $\theta = 110^\circ$ the upper cap is again the larger. It now helps to consider small free caps as a perturbation from a state in which both bubbles have completely clogged surfaces ($\alpha = \beta = 180^\circ$). The upper bubble's small free cap is in a region of faster flow than the lower bubble's (figure 4c), it can be smaller and have the same effect on the drag, and hence the upper stagnant cap is larger.

If the bubbles are sufficiently close and their caps sufficiently large, figure 2 would suggest that the caps can be of very different sizes. However figure 5, which is a plot

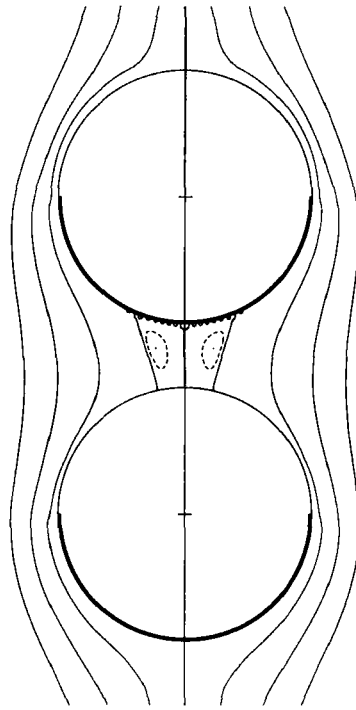


FIGURE 5. Streamline plot for $\alpha = \beta = 90^\circ$, $s = 2.5$, with streamlines dotted in the back-eddy. (The very small closed loops near the bottom of the upper bubble are numerical artefacts.)

α	β	s
0	0	2.0
30	29.45	2.5
60	62.09	2.8
90	91.31	3.0
120	118.76	3.2
150	144.81	3.4
180	180.00	3.6

TABLE 1. Lower cap angle β (in degrees) and separation s (in bubble radii) as a function of upper cap angle α for a pair of bubbles with incipient eddies and equal drag coefficients

of selected streamlines for $s = 2.5$, $\alpha = \beta = 90^\circ$, reminds us that in such cases there is at least one closed eddy on the upper cap and the present theory would not apply. (Each stagnation point where the flow is towards a bubble would be in a shear-free region and each stagnation point where the flow is away from a bubble would be in a stagnant region, and the bubble surfaces would be divided into several free and stagnant zones.) For a range of values of α we found the values of β and s for which the drag coefficients were equal and eddies were about to appear (table 1). Figure 5 explains why the s values are given to only two significant figures: if the true eddy is very small it is hard to distinguish from the spurious eddies which appear on the upper bubble's cap and are an artefact of truncating the series (25). Figure 5 also shows that streamlines close to the surface are much further from it over the cap than

over the free part; this is of course because the velocity is zero on the cap and small near it.

The first main item of new physics in this paper is the relation between the cap sizes α, β for equal drag, with its (at first) surprising reversals in the sign of $\alpha - \beta$, which can be understood qualitatively and calculated quantitatively as shown above.

The second is the surfactant-induced interaction between bubbles. If s is large or the caps are small, there is too much surfactant on the lower bubble for the equal-drag relation to be satisfied, so that the upper one rises faster. We conjecture that this will still happen if s is smaller or the caps are not small (except of course for 180° caps, for which the speeds are known to be equal, by symmetry about the horizontal plane halfway between the bubbles). To confirm (or refute) this conjecture we need good numerical results for the surface velocity and shear stress, which are not yet available.

We are grateful to Dr John Hinch whose questions about the front stagnation region of the second bubble made us devise the theory of §5.2, and to the referees who showed us where various other parts of this paper needed clarifying. J.F.H. also wishes to thank the Victoria University of Wellington for research leave, and the Mathematical Institute, Oxford, for hospitality and facilities while this paper was being revised.

REFERENCES

- ADAM, N. K. 1968 *The Physics and Chemistry of Surfaces*. Dover.
- BATEMAN MANUSCRIPT PROJECT 1954 *Tables of Integral Transforms*, vol. 2. McGraw-Hill.
- CARSLAW, H. S. & JAEGER, J. C. 1959 *Conduction of Heat in Solids*. Oxford University Press.
- CLIFT, R., GRACE, J. R. & WEBER, M. E. 1978 *Bubbles, Drops and Particles*. Academic.
- COLLINS, W. D. 1961 On some dual integral series equations and their application to electrostatic problems for spheroidal caps. *Proc. Camb. Phil. Soc.* **57**, 367–384.
- DAVIS, A. M. J., O'NEILL, M. E., DORREPAAL, J. M. & RANGER, K. B. 1976 Separation from the surface of two equal spheres in Stokes flow. *J. Fluid Mech.* **77**, 625–644.
- DAVIS, R. E. & ACRIVOS, A. 1966 The influence of surfactants on the creeping motion of bubbles. *Chem. Engng Sci.* **21**, 681–685.
- GLUCKMAN, M. J., PFEFFER, R. & WEINBAUM, S. 1971 A new technique for treating multiparticle slow viscous flow: axisymmetric flow past spheres and spheroids. *J. Fluid Mech.* **50**, 705–740.
- HARPER, J. F. 1970 On bubbles rising in line at large Reynolds numbers. *J. Fluid Mech.* **41**, 751–758.
- HARPER, J. F. 1972 The motion of bubbles and drops through liquids. *Adv. Appl. Mech.* **12**, 59–129.
- HARPER, J. F. 1973 On bubbles with small adsorbed films rising in liquids at low Reynolds numbers. *J. Fluid Mech.* **58**, 539–545.
- HARPER, J. F. 1974 On spherical bubbles rising slowly in dilute surfactant solutions. *Q. J. Mech. Appl. Maths* **27**, 87–100.
- HARPER, J. F. 1982 Surface activity and bubble motion. *Appl. Sci. Res.* **38**, 343–352.
- HARPER, J. F. 1983 Axisymmetric Stokes flow images in spherical surfaces with applications to rising bubbles. *J. Austral. Math. Soc.* **B25**, 217–231.
- HARPER, J. F. & DIXON, J. N. 1974 The leading edge of a surface film on contaminated flowing water. *Proc. 5th Australasian Conf. Hydraulics Fluid Mech. Christchurch, NZ*, vol. 2, pp. 499–505.
- LERNER, L. 1985 *The interaction of surface-contaminated drops in Stokes flow*. MSc thesis, Victoria University of Wellington, NZ.

- LEVAN, M. D. & HOLBROOK, J. A. 1989 Motion of a droplet containing surfactant. *J. Colloid Interface Sci.* **131**, 242–251.
- LEVICH, V. G. 1962 *Physicochemical Hydrodynamics*. Prentice-Hall.
- LIGHTHILL, M. J. 1950 Contributions to the theory of heat transfer through a laminar boundary layer. *Proc. R. Soc. Lond. A* **202**, 359–377.
- NONWEILER, T. R. F. 1984 *Computational Mathematics*. Chichester: Ellis Horwood and New York: Halsted Press.
- PAIS, A. 1982 '*Subtle is the Lord ...*'. Oxford University Press.
- PAYNE, L. E. & PELL, W. H. 1960 The Stokes flow problem for a class of axially symmetric bodies. *J. Fluid Mech.* **7**, 529–549.
- PRUPPACHER, H. R. & KLETT, J. D. 1978 *Microphysics of Clouds and Precipitation*. Reidel.
- RUSHTON, E. & DAVIES, G. A. 1978 The slow motion of two spherical particles along their line of centers. *Intl J. Multiphase Flow* **4**, 357–381.
- SADHAL, S. S. & JOHNSON, R. E. 1983 Stokes flow past bubbles and drops partially coated with thin films. Part 1. Stagnant cap of surfactant film – exact solution. *J. Fluid Mech.* **126**, 237–250.
- SANSONE, G. 1959 *Orthogonal Functions*. Interscience.
- SAVIC, P. 1953 Circulation and distortion of liquid drops falling through a viscous medium. *Natl Res. Council. Can., Div. Mech. Engng Rep.* MT-22.
- WACHOLDER, E. & WEIHS, D. 1972 Slow motion of a fluid sphere in the vicinity of another sphere or a plane boundary. *Chem. Engng Sci.* **27**, 1817–1828.